sciendo

*Polish Journal of Chemical Technology, 26, 3, 16—20, 10.2478/pjct-2024-0025*

# Synthesis and Self-assembly of a Simple $CO_2$-responsive Diblock Polymer

**Pengfei Zhang [1*], Xianwu Jing[1, 2*], Lang Zhou[3], Qiang Liu[3], Yadong Zhang[1]**

[1]Research Institute of Natural Gas Technology, PetroChina Southwest Oil and Gasfield Company, Chengdu, Sichuan, 610213, People's Republic of China
[2]Shale Gas Evaluation and Exploitation Key Laboratory of Sichuan Province, Sichuan Provincial Department of Science and Technology, Chengdu, Sichuan, 610051, People's Republic of China
[3]Engineering Technology Department, PetroChina Southwest Oil and Gasfield Company, Chengdu, Sichuan, 610081, People's Republic of China
[*]*Corresponding authors: e-mail:* zhangpf2020@petrochina.com.cn, jingxw2018@petrochina.com.cn

Methoxypolyethylene glycol 1900 and α-bromoisobutanoyl bromide were utilized for alcoholysis reaction to obtain a macromolecular initiator. Then, a simple amphiphilic diblockpolymer (mPEG-PDMAEMA) based on the initiator and dimethylaminoethyl methacrylate was synthesized through the atomic transfer radical polymerization (ATRP) method. The structures of the initiator and diblock polymer were accurately characterized using infrared spectrum and proton nuclear magnetic resonance spectroscopy ($^1$H NMR). Cryo-transmission electron microscopy revealed the self-assembly of mPEG-PDMAEMA into vesicle-like structures in water. Upon injection of $CO_2$ into the solution, the tertiary amine structure within PDMAEMA underwent protonation, resulting in the mPEG-PDMAEMA adopting a hydrophilic structure. Consequently, the vesicles dissociated and dispersed, forming a network-like structure in water. The protonation phenomenon was confirmed by $^1$H NMR, as evidenced by the shifting of alkyl hydrogen atoms near nitrogen atoms toward downfield positions.

**Keywords:** ATRP; diblock polymer; vesicles; protonation.

## INTRODUCTION

The advancement of block polymers holds significant importance in both academic research and practical applications[1–3]. Leroux[4] et al. presented a novel preparation of polymer micelles, which includes insoluble anti-tumor drugs. They utilized a block polymer consisting of methoxy polyethylene glycol polyester (D, L-lactide, L-lactide, caprolactone, or glycolide) to encapsulate paclitaxel or docetaxel, thereby achieving targeted drug delivery. Similarly, Gong et al.[5] also introduced polymer micelles with similar structures, which could achieve targeted drug delivery. These studies have now reached clinical applicability, and polymer micelles have been employed in the adjuvant treatment of tumors. For instance, the commercially available polymeric micellar paclitaxel for injection is a new nanodrug delivery, that combines methoxypolyethylene glycol polylactic acid amphiphilic diblock copolymer (mPEG-PDLLA) with the anticancer drug paclitaxel. Its mechanism involves the use of micelles formed by mPEG-PDLLA to encapsulate and transport paclitaxel to the tumor site for efficient treatment[6–8].

From the above, it is evident that the key aspect of targeted drug delivery is the development of block polymers with appropriate structures capable of forming vesicles[9, 10]. These vesicles enable the encapsulation of drugs and facilitate targeted release at the site of the lesion. Previous reports indicate that tumor location exhibits heightened metabolism, resulting in elevated heat and $CO_2$ production compared to normal areas[11–13]. In this study, we focused on the synthesis of a simple diblock polymer called mPEG-PDMAEMA, achieved by combining methoxy polyethylene glycol (mPEG) and dimethylamine methacrylate (DMAEMA) via atomic transfer radical polymerization (ATRP)[14–16]. This diblock polymer forms vesicular micelles in an aqueous environment, which disintegrate in the presence of $CO_2$. Such a diblock polymer shows promise for application in drug delivery.

## EXPERIMENTAL MATERIALS AND METHOD

Methoxypolyethylene glycol (mPEG) with a molecular weight of approximately 1900, α-bromoisobutyryl bromide (BIBB), calcium hydride ($CaH_2$), dimethylaminoethyl methacrylate (DMAEMA), copper bromide (CuBr), potassium bromide (KBr), deuterated water ($D_2O$) and N,N,N',N'',N''-pentamethyldiethylenetriamine (PMDETA), all of which were of AR grade and purchased from Shanghai Aladdin Biochemical Technology Co., Ltd. Additionally, dichloromethane (DCM), triethylamine (TEA), sodium bicarbonate ($NaHCO_3$), hydrochloric acid (HCl, 36%), and acetic acid, all of which were of AR grade and purchased from Kelong Chemical Co., Ltd. (China). DCM was redistillated to remove trace moisture by using $CaH_2$ as a dehydrating agent, the heating temperature was maintained at 45±1 °C. CuBr was washed repeatedly with acetic acid and ethanol, followed by evaporation and drying to obtain a white powder, and then stored in a reagent bottle filled with $N_2$ for future use.

The dialysis bag (Beijing Mengyimei Biotechnology Co., Ltd.) was boiled in pure water for 10 minutes and then allowed to cool naturally, and then stored in water for later use.

The infrared spectrometer, specifically the Nicolet iS 10 model manufactured by Thermo Fisher Scientific (USA), was used to analyze the molecular structure of the sample. This analysis was conducted by scanning a wavelength range of 4000~500 $cm^{-1}$ using a KBr tablet. To achieve precise characterization of the molecular structure of macromolecule initiator and polymer, a small quantity of samples was mixed with $D_2O$ within a nuclear magnetic tube. This mixture was then subjected to analysis using a nuclear magnetic resonance spectrometer, specifically the Bruker 400 MHz model (Switzerland). To ensure accuracy, an internal standard substance tetramethylsilane (TMS) was used.

Additionally, the high-resolution transmission electron microscope by Japan Electronics Co., Ltd. and a capillary viscometer with an inner diameter of 0.8 mm from Shanghai Liangjing Glass Instrument Factory were employed. Approximately 5 μL of the sample solution was placed on a TEM copper grid. Next, any excess solution was removed by using filter paper to create a liquid film. Subsequently, the sample was rapidly transferred into liquid ethane that was cooled by liquid nitrogen to a temperature of –165 °C. This freezing process ensures that the substances within the solution retain their original state and are instantly frozen. To analyze the sample, the JEM-2010 (120 kV) from Japan Electronics Corporation was employed, while the test results were collected using the Gatan Multiscan charge-coupled device camera. The mPEG-PDMAEMA aqueous solution with a concentration of 0.5% was prepared. Subsequently, the time it takes for the solution to flow out was measured using a capillary viscometer from Shanghai Liangjing Glass Instrument Factory. This enabled the calculation of the kinematic viscosity. The experiment was conducted in a water bath maintained at a temperature of 25 °C.

### Synthesis of Macromolecular Initiators

Firstly, 20 g of mPEG (0.01 mol) was dissolved in 80 mL of DCM. The resulting solution was transferred into a dry flask and placed in an ice bath. Next, 20 mL DCM solution with 2.53 g of BIBB (0.011 mol) was slowly added, while the solution was stirred for 10 minutes. Subsequently, a 50 mL DCM solution containing 1.53 g of TEA (0.015 mol) was gradually introduced into the mixture and it was removed from the ice bath. The mixture was stirred for 12 hours at room temperature. The precipitate was filtered and the remaining liquid was poured through a separating funnel. The mixture was washed three times with 1% solution of $NaHCO_3$ and 1% dilute hydrochloric acid solution. The lower DCM solution was then separated and then, the macromolecular initiator mPEG-Br was obtained by vacuum drying. The structure of mPEG-Br was determined using IR and NMR analysis.

#### *Synthesis and Purification of Diblock Polymer*

Distilled water (50 g) was poured into a clean flask, and while stirring, $N_2$ gas was slowly and continuously introduced for 30 minutes. Then, 0.5 g of mPEG-Br and 10 g of DMAEMA were added. Next, 0.005 g of the white powder CuBr was measured and added to the flask. The mixture was stirred thoroughly until the powder was evenly dispersed. An amount of PMDETA 0.05 g was introduced using a sampler while continuing to slowly introduce $N_2$ bubbles. Over time, the solution gradually turned blue. After a reaction time of 6 hours, the flow of $N_2$ was stopped and the cap was removed from the flask's opening. The resulting blue gel was transferred into a dialysis bag and securely sealed. The bag was then submerged in distilled water for 48 hours, and the water was frequently changed during the dialysis process. Finally, the colorless and viscous solution was extracted from the dialysis bag. The final polymer mPEG--PDMAEMA can be obtained under vacuum drying. The synthesis pathway is depicted in Fig. 1.

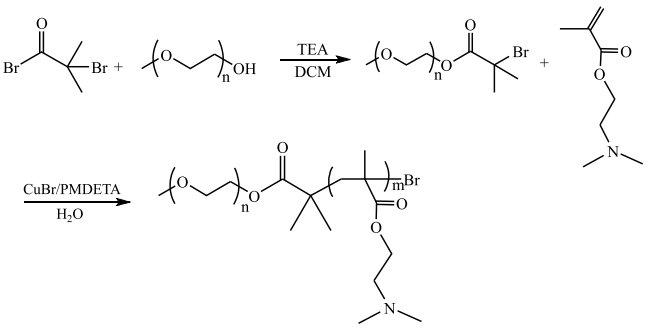


**Figure 1.** Synthesis route of macromolecular initiator diblock polymer mPEG-PDMAEMA

## RESULTS AND DISCUSSION

### Characterization of Macromolecular Initiator and Diblock Polymer

The IR spectrum of the macromolecule initiator and raw materials is depicted in Fig. 2. The final product is called α-bromo isobutyric acid polyethylene glycol methyl ether ester, which is abbreviated as mPEG-Br.

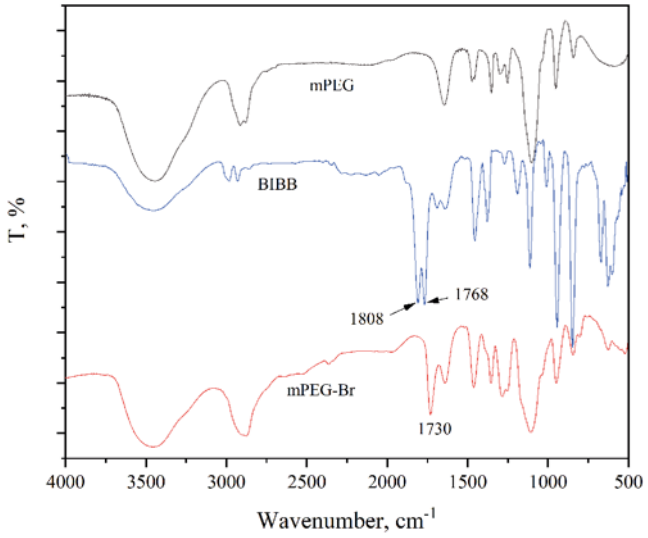


**Figure 2.** IR of mPEG-Br and reactants

Fig. 2 illustrates a comparison of infrared characteristic peaks. The peaks of BIBB at 1801 $cm^{-1}$ and 1763 $cm^{-1}$ are notable, as they correspond significantly to the acyl bromine carbonyl absorption peak in terms of frequency. The Fermi vibration, which is associated with stretching vibrations of carbonyl C=O and C-Br[17, 18], causes the absorption peak of carbonyl groups to split into double peaks. In contrast to mPEG, mPEG-Br displays a distinct absorption peak at 1728 $cm^{-1}$, indicating the presence of an ester carbonyl group[19]. Furthermore, there is no characteristic peak of BIBB (1801 $cm^{-1}$ and 1763 $cm^{-1}$) in mPEG-Br, indicating the successful production of macromolecular initiator mPEG-Br with high purity and no residual of BIBB.

#### *Nuclear Magnetic Hydrogen Spectrogram of the Polymer*

Additionally, mPEG-Br was precisely characterized using $^1H$ NMR, and the molecular structural formula of mPEG-Br was accurately determined by analyzing the peak area.

The $^1H$ NMR spectrum of mPEG-Br in Fig. 3 shows the following shifts: the shift range from 4.363 to 4.282 ppm

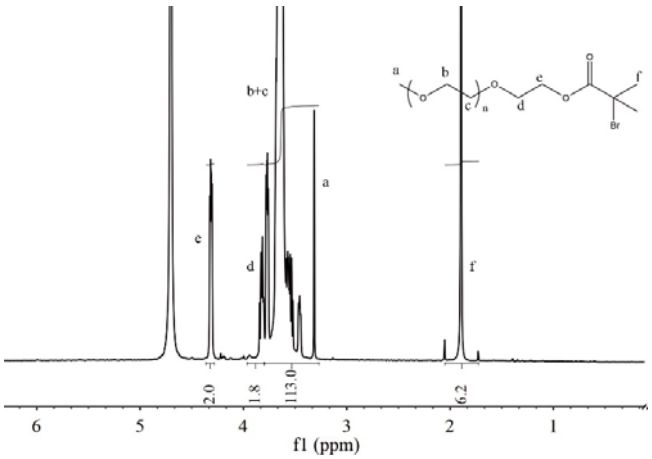


**Figure 3.** $^1$H NMR of mPEG-Br (400 MHz, $D_2O$, ppm)

corresponds to the hydrogen atoms in the α-methylene group linked to the ester, peak e, -$CH_2$-C$\boldsymbol{H_2}$-C=O. The shift range from 3.964 to 3.801 ppm corresponds to the hydrogen atoms in the β-position of the ester linkage, peak d, -C$\boldsymbol{H_2}$-$CH_2$-C=O. The shift range from 3.795 to 3.269 ppm is attributed to the hydrogen atoms in both the methylene and terminal methyl groups of the polyoxyethylene chain, peak b+c and peak a, -O-C$\boldsymbol{H_2}$-C$\boldsymbol{H_2}$-O- and -O-C$\boldsymbol{H_3}$. The shift range from 2.050 to 1.723 ppm is attributed to the hydrogen atoms in the α-methyl group linked to the bromine atom, peak f, Br--C-(C$\boldsymbol{H_3}$)$_2$. By analyzing the integrated areas of the $^1$H NMR spectrum, it can be determined that the number of repeated units in the polyoxyethylene ether chain of mPEG-Br is 30, the actual molecular weight of mPEG should be about 1350.

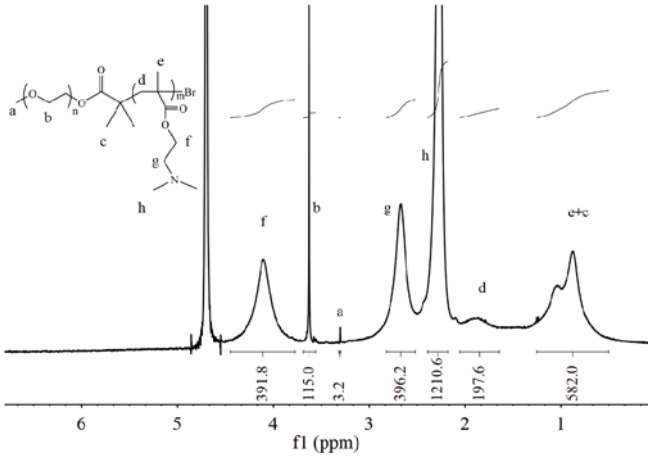


**Figure 4.** $^1$H NMR of mPEG-PDMAEMA (400 MHz, $D_2O$, ppm)

The $^1$H NMR spectroscopy results in Fig. 4 can be summarized as follows: peaks in the range of 4.443 to 3.769 ppm are attributed to the hydrogen atoms in the α position of the ester group in DMAEMA, peak f, O=C-C$\boldsymbol{H_2}$-$CH_2$-. Peaks in the range of 3.689 to 3.556 ppm are attributed to the hydrogen atoms in the polyoxyethylene chain, peak b, -O-C$\boldsymbol{H_2}$-C$\boldsymbol{H_2}$-O-. A peak at 3.318 to 3.298 ppm is attributed to the-C$\boldsymbol{H_3}$ on the end group of mPEG, peak a. Peaks in the range of 2.821 to 2.520 ppm are attributed to the hydrogen atoms on methylene in DMAEMA, peak g, O=C-$CH_2$-C$\boldsymbol{H_2}$-. Peaks in the range of 2.388 to 2.179 ppm are attributed to the methyl hydrogen atom connected to the nitrogen atom in DMAEMA, peak h, -N-(C$\boldsymbol{H_3}$)$_2$. Peaks in the range of 2.053 to 1.645 ppm are attributed to the hydrogen atoms in the backbone chain of the polymerization, peak d, -C$\boldsymbol{H_2}$-C-. Peaks in the range of 1.249 to 0.502 ppm are attributed to the methyl hydrogen atoms connected to the backbone chain of the polymerization, peak e+c, -C$\boldsymbol{H_3}$. The integral areas of the peaks indicate that peak a and peak b correspond to the hydrogen atoms in the initiator, and the integral areas align with theoretical expectations (see Fig. 3). The integral areas of peaks f, g, h, d, and the sum of e and c are equal to the number of hydrogen atoms in the corresponding group in DMAEMA, allowing for the calculation of the number of repeated units in DMAEMA, which is determined to be 200. Thus, the resulting diblock polymer structure formula is $mPEG_{30}$-$PDMAEMA_{200}$, and the molecular weight is approximately 32850 g/mol. Additionally, we can infer from the molecular weight that the conversion rate of DMAEMA is estimated to be approximately 78%.

**Cryo-transmission Electron Microscopy Analysis**

Cryo-transmission electron microscopy revealed the presence of 0.5% mPEG-PDMAEMA in water. The findings obtained are outlined below.

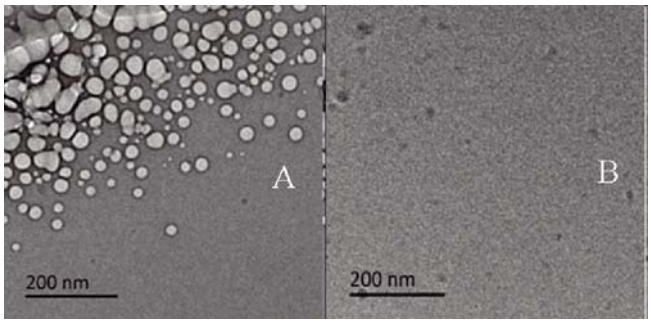


**Figure 5.** Self-assembly morphology of mPEG-PDMAEMA in aqueous solution before (A) and after (B) bubbling $CO_2$

As shown in Fig. 5, when a 0.5% aqueous solution of mPEG-PDMAEMA is dissolved in water, it undergoes self-assembly and forms vesicle structures (Fig. 5A). Upon injecting $CO_2$ into the solution, the vesicles break apart and transform into a complex network structure (Fig. 5B). This change in morphology indicates that the desired substance can be pre-encapsulated within the vesicles, which can later disintegrate upon reaching the appropriate location or when environmental conditions change. As a result, the enclosed substance is released, demonstrating potential applications in targeted drug delivery.

**Mechanism Interpretation**

Due to its composition as a hydrophilic-hydrophobic diblock polymer, mPEG-PDMAEMA exhibits an amphiphilic naturally[20, 21]. This characteristic allows the polymer to function as a surfactant, forming vesicles when placed in water. When $CO_2$ is introduced into the solution, the tertiary amine in PDMAEMA reacts with carbonic acid, resulting in the formation of a tertiary amine salt. Consequently, mPEG-PDMAEMA transforms a fully hydrophilic structure, causing the vesicles

to dissociate and form a network structure within the water. The protonation process is confirmed through $^1$H NMR analysis, and the transformation of the structural formula is depicted in Fig. 6.

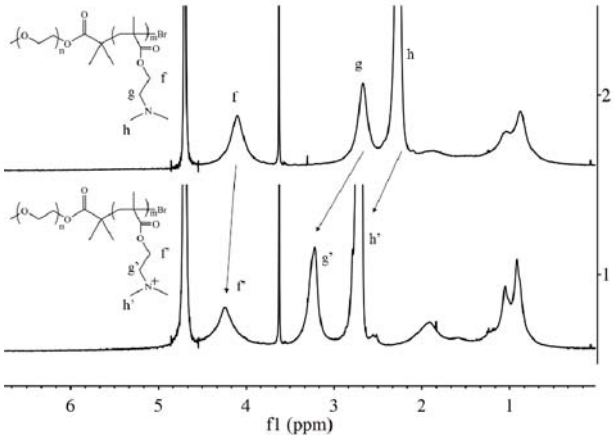


**Figure 6.** Comparison of $^1$H NMR spectra of mPEG-PDMAEMA before (2) and after (1) protonation

Upon protonation, the hydrogen atom in methyl which is connected to the nitrogen atom undergoes a downfield from 4.1 ppm to 4.2 ppm (f→f'). Similarly, the hydrogen atom connected to α-methylene which is attached to the nitrogen atom experiences a downshift from 2.7 ppm to 3.2 ppm (g→g'). Additionally, the hydrogen atom connected to the β-methylene which is attached to the nitrogen atom moves from 2.3 ppm to 2.7 ppm (h→h'). This evidence supports the conclusion that the tertiary amine transforms into a tertiary amine salt through this process.

### Viscosity Change

Based on the experiments, it can be deduced that the self-assembly morphology of the mPEG-PDMAEMA solution underwent substantial changes before and after the introduction of $CO_2$. These changes have the potential to alter the macroscopic properties of the solution. To assess this, the viscosity of a 0.5% mPEG-PDMAEMA solution was measured using the capillary viscosity method before and after exposure to $CO_2$. Following $CO_2$ injection, $N_2$ was introduced into the solution to remove the $CO_2$, and the restoration of solution performance was confirmed.

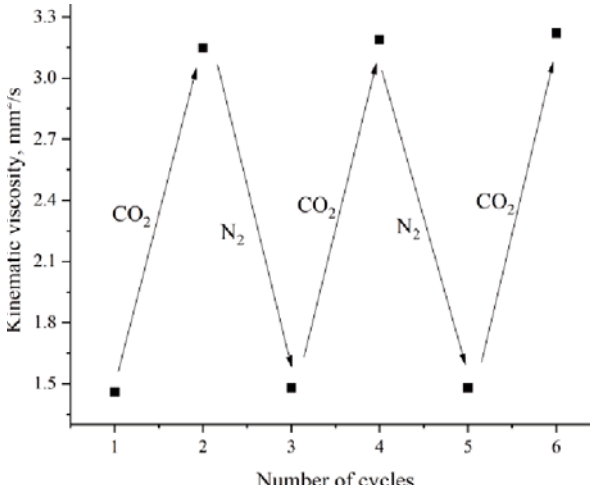


**Figure 7.** Viscosity of mPEG-PDMAEMA solution after circulating $CO_2$ and $N_2$

As shown in Fig. 7, the viscosity of the solution increased from 1.46 mm$^2$/s to 3.15 mm$^2$/s when $CO_2$ was injected into mPEG-PDMAEMA. This increase in viscosity aligned with the morphological changes observed in mPEG-PDMAEMA shown in Fig. 5. Subsequently, when $N_2$ was reintroduced into the solution, the viscosity returned to 1.49 mm$^2$/s. This change indicated that the process of deprotonation occurred, converting the tertiary amine salt back into tertiary amine. This experiment demonstrated the reversible nature of protonation and deprotonation in mPEG-PDMAEMA, allowing the self-assembled morphology to switch between vesicles and reticular structures with ease.

## CONCLUSIONS

An alcoholysis method was employed to synthesize a macromolecule initiator, while the atomic transfer radical polymerization method was used to synthesize an amphiphilic diblock polymer called mPEG-PDMAEMA. The initiator and diblock polymer underwent characterization through IR and $^1$H NMR. By utilizing transmission electron microscopy, it was observed that 0.5% of the mPEG-PDMAEMA formed vesicles in aqueous environment. However, when $CO_2$ was introduced into the solution, the vesicles disintegrated. This phenomenon can be attributed to the protonation of the tertiary amine present in PDMAEMA, resulting in the formation of a tertiary amine salt. Consequently, mPEG-PDMAEMA transformed from an amphiphilic structure to a fully hydrophilic structure. The protonation process was verified using $^1$H NMR.

### Funding

This work was supported by Major Engineering Technology Field Test Project of CNPC (NO. 2019F-31) and Scientific Research, Technological Development Project of PetroChina (NO. 2022CGCGZ005) and Southwest Oil and Gas Field Company Scientific Research Project (NO. 20230302-14). The funding body played no role in the design of the study and collection, analysis, interpretation of data, and in writing the manuscript.

## LITERATURE CITED

1. Bates, C.M. & Bates, F.S. (2017). 50th Anniversary Perspective: Block Polymers Pure Potential. *Macromolecules* 50, 3–22 DOI: 10.1021/acs.macromol.6b02355.

2. Hasannia, M., Aliabadi, A., Abnous, K., Taghdisi, S.M., Ramezani, M. & Alibolandi, M. (2022). Synthesis of Block Bopolymers Used in Polymersome Fabrication: Application in Drug Delivery. *J. Control Release* 341, 95–117 DOI: 10.1016/j.jconrel.2021.11.010.

3. Xu, L., Zhang, X., Chu, Z., Wang, H., Li, Y., Shen, X., Cai, L., Shi, H., Zhu, C. & Pan, J. (2021). Temperature-responsive Multilayer Films Based on Block Copolymer-coated Silica Nanoparticles for Long-term Release of Favipiravir. *Acs Appl. Nano. Mater.* 4, 14014–14025 DOI: 10.1021/acsanm.1c03334.

4. Gaucher, G., Marchessault, R.H. & Leroux, J. (2010). Polyester-based Micelles and Nanoparticles for the Parenteral Delivery Of Taxanes. *J. Controll. Release* 143, 2–12. DOI: 10.1016/j.jconrel.2009.11.012.

5. Gong, F., Cheng, X., Wang, S., Wang, Y., Gao, Y. & Cheng, S. (2009). Biodegradable Comb-dendritic Tri-block Copolymers Consisting of Poly(ethylene Glycol) and Poly(l-lactide): Synthesis, Characterizations, and Regulation of Surface

Morphology and Cell Responses. *Polymer* 50, 2775–2785. DOI: 10.1016/j.polymer.2009.04.033.

6. Zhang, X., Burt, H.M., Mangold, G., Dexter, D., Von, Hoff, D., Mayer, L. & Hunter, W.L. (1997). Anti-tumor Efficacy and Biodistribution of Intravenous Polymeric Micellar Paclitaxel. *Anti-Cancer Drugs* 8, 696–701. DOI: 10.1097/00001813-199708000-00008.

7. Gong, C., Xie, Y., Wu, Q., Wang, Y., Deng, S., Xiong, D., Liu, L., Xiang, M., Qian, Z. & Wei, Y. (2012). Improving Anti-tumor Activity with Polymeric Micelles Entrapping Paclitaxel in Pulmonary Carcinoma. *Nanoscale* 4, 6004–6017. DOI: 10.1039/C2NR31517C.

8. Shi, M., Sun, J., Zhou, J., Yu, H., Yu, S., Xia, G., Wang, L., Teng, Y., Liu, G. & Yu, C. (2018). Phase I dose Escalation and Pharmacokinetic Study on the Nanoparticle Formulation of Polymeric Micellar Paclitaxel for Injection in Patients with Advanced Solid Malignancies. *Invest. New Drugs* 36, 269–277 DOI: 10.1007/s10637-017-0506-4.

9. Onaca, O., Enea, R., Hughes, D.W. & Meier, W. (2009). Stimuli-responsive Polymersomes as Nanocarriers for Drug and Gene Delivery. *Macromol. Biosci.* 9, 129–139. DOI: 10.1002/mabi.200800248.

10. Hamidi, M., Shahbazi, M.A. & Rostamizadeh, K. (2012). Copolymers: Efficient Carriers for Intelligent Nanoparticulate Drug Targeting and Gene Therapy. *Macromol. Biosci.* 12, 144–164. DOI: 10.1002/mabi.201100193.

11. Hegyi, G., Szigeti, G.P., Szász, A. & Jia, W. (2013). Hyperthermia versus Oncothermia: Cellular Effects in Complementary Cancer Therapy. *Evid-Based Compl. Alt. Med.* 2013, 672873. DOI: 10.1155/2013/672873.

12. Krieg, R., C., Knuechel, R., Schiffmann, E., Liotta, L.A., Petricoin, III EF. & Herrmann, P.C. (2004). Mitochondrial Proteome: Cancer-altered Metabolism Associated with Cytochrome *c* oxidase Subunit Level Variation. *Proteomics* 4, 2789–2795. DOI: 10.1002/pmic.200300796.

13. Kir, S., Komaba, H., Garcia, A.P., Economopoulos, K.P., Liu, W., Lanske, B., Hodin, R.A. & Spiegelman, B.M. (2016). PTH/PTHrP Receptor Mediates Cachexia in Models of Kidney Failure and Cancer. *Cell Metab.* 23, 315–323. DOI: 10.1016/j.cmet.2015.11.003.

14. Matyjaszewski, K. (2012). Atom transfer radical polymerization (ATRP): Current Status and Future Perspectives. *Macromolecules* 45, 4015–4039 DOI: 10.1021/ma3001719.

15. Wang, J., M. & Matyjaszewski, K. (1995). " Living"/controlled Radical Polymerization. Transition-metal-catalyzed Atom Transfer Radical Polymerization in the Presence of a Conventional Radical Initiator. *Macromolecules* 28, 7572–7573 DOI: 10.1021/ma00126a041.

16. Wang, J. & Matyjaszewski, K. (1995). Controlled/"Living" Radical Polymerization. Halogen Atom Transfer Radical Polymerization Promoted by a Cu(I)/Cu(II) Redox Process. *Macromolecules* 28, 7901–7910. DOI: 10.1021/ma00127a042.

17. Brito, A.L.B., Lopes, S., Ogruc, Ildiz, G. & Fausto, R. (2023). Structure, Vibrational Spectra, and Cryogenic MatrixPhotochemistry of 6-Bromopyridine-2-carbaldehyde: From the Single Molecule of the Compound to the Neat Crystalline Material. *Molecules* 28, 1673. DOI: 10.3390/molecules28041673.

18. Dostert, K., O'Brien, CP., Liu, W., Riedel, W., Savara, A., Tkatchenko, A., Schauermann, S. & Freund, H. (2016). Adsorption of Isophorone and Trimethyl-cyclohexanone on Pd (111): A Combination of Infrared Reflection Absorption Spectroscopy and Density Functional Theory Studies. *Surf. Sci.* 650, 149–160. DOI: 10.1016/j.susc.2016.01.026.

19. Premadasa, U.I., Adhikari, N.M. & Cimatu, K.L.A. (2019). Molecular Insights into the Role of Electronic Substituents on the Chemical Environment of the $-CH_3$ and $>C{=}O$ Groups of Neat Liquid Monomers Using Sum Frequency Generation Spectroscopy. *The J. Phys. Chem. C* 123, 28201–28209 DOI: 10.1021/acs.jpcc.9b07816.

20. Wu, J.D., Zhang, C., Jiang, D., J., Zhao, S., F., Jiang, Y., L., Cai, G., Q. & Wang, J., P. (2016). Self-cleaning pH/thermo-responsive Cotton Fabric with Smart-control and Reusable Functions for Oil/water Separation. *RSC. Adv.* 6, 24076–24082. DOI: 10.1039/C6RA02252A.

21. Liang, L., Dong, Y., Wang, H. & Meng, X. (2019). Smart Cotton Fabric with $CO_2$-Responsive Wettability for Controlled Oil/Water Separation. *Adv. Fiber Mater.* 1, 222–230. DOI: 10.1007/s42765-019-00018-7.